Environmental Science & Technology

pubs.acs.org/est

Article

Target and Nontarget Analysis of Per- and Polyfluoralkyl Substances in Wastewater from Electronics Fabrication Facilities

Paige Jacob, Krista A. Barzen-Hanson, and Damian E. Helbling*

Cite This: *Environ. Sci. Technol.* 2021, 55, 2346−2356

Read Online

ACCESS | Metrics & More | Article Recommendations | Supporting Information

ABSTRACT: The goals of this study were to improve our understanding of the types of per- and polyfluoroalkyl substances (PFASs) that occur in wastewater from electronics fabrication facilities (fabs) and to assess the relative concentrations of PFAS species. We collected wastewater samples from three fabs in the United States, analyzed the samples by means of high-resolution mass spectrometry, and implemented complementary target and nontarget analyses. Twelve of 25 target PFASs were quantified in at least one sample, and five perfluorocarboxylates and perfluorobutane sulfonate (PFBS) were quantified in all samples. PFBS was quantified at the highest concentration among the samples (8040 ng L^{-1}) and we expect that its presence is related to the use of photoacid generators during photolithography. The sum concentrations of the target PFASs in the diluted discharge samples from each fab were 623, 394, and 376 ng L^{-1}. Nontarget analysis revealed the presence of 41 homologous series of PFASs comprising 133 homologues. We proposed structures for 15 homologous series of nontarget PFASs, six of which are reported here for the first time. Using an approach for semiquantification of nontarget PFASs, we estimated that the sum concentrations of target and nontarget PFASs in the diluted discharge samples from each fab were 1490, 78 700, and 2170 ng L^{-1}. Our findings are essential for developing alternative photolithography chemicals or informing the implementation of advanced wastewater treatment technologies at fabs.

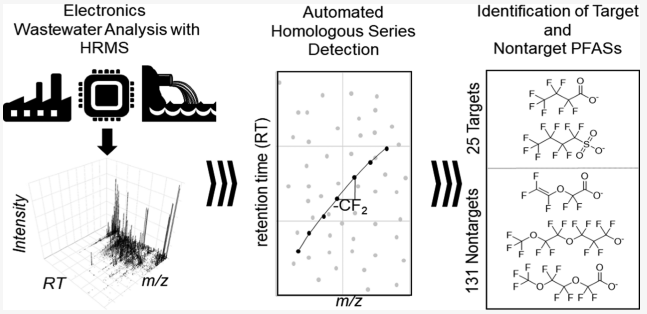

INTRODUCTION

Per- and polyfluoroalkyl substances (PFASs) are ubiquitous environmental contaminants with a variety of known and unknown sources.[1−3] PFASs are used commercially and industrially as flame retardants, grease repellants, waterproofing agents, and surfactants.[4] The thermal and chemical stability of PFASs make them persistent in the environment,[5] and a number of studies have demonstrated adverse ecological and human health effects including bioaccumulation,[6] cancer,[7] immunotoxicity,[8] and developmental toxicity.[9] The major known sources of PFASs in the environment include aqueous film-forming foam (AFFF) products,[10] landfill leachate,[11] municipal wastewater treatment plant effluent,[12] and discharges from manufacturing facilities including chrome plating, plastics, and fluorochemical production plants.[13−15]

The electronics manufacturing industry is an understudied, yet potentially important, source of known and unknown PFASs in the environment.[16] Electronics fabrication facilities, or fabs, produce electronics products from substrates by means of nanofabrication and photolithography. Photolithography is a process used to transfer a pattern from a photomask to a photosensitive chemical photoresist applied on the surface of a substrate.[17] The substrate is exposed to UV radiation to make patterns that provide specific functional properties.[18] PFASs can be constituents of photoresists and related photolithography chemical mixtures, including antireflective coatings.[18,19] For example, perfluorobutane sulfonate (PFBS) is a known constituent of photoacid generators[20] and a variety of fluorotelomer-based acrylate polymers (FTACPs) are listed on safety data sheets (SDSs) of commercially available photoresists.[4,18,21] The extent to which these types of PFASs and their transformation products[22−26] occur in aqueous wastewater discharged from fabs is unknown.

The emerging approach to evaluating PFASs from previously unexplored sources is to implement complementary target and nontarget analyses.[27] Target analyses aim to quantify the occurrence of known PFASs by means of high-performance liquid chromatography (HPLC) and mass spectrometry. Analytical methods currently available for industrial wastewater enable sensitive quantification of dozens of individual PFAS species with limits of detection in the low nanogram per liter range.[28,29] Nontarget analyses aim to more fully elucidate the types of PFASs that are present in a sample, including PFASs that are unexpected or unknown, by means of high-resolution

Received: October 4, 2020
Revised: December 14, 2020
Accepted: January 18, 2021
Published: January 26, 2021

https://dx.doi.org/10.1021/acs.est.0c06690
Environ. Sci. Technol. 2021, 55, 2346−2356

mass spectrometry (HRMS).[30] Recent studies have employed HRMS to more comprehensively characterize PFASs in AFFF-contaminated groundwater[31] and other sources.[32,33] The general approach relies on data-mining techniques to discover evidence of fluorinated compounds, which can be prioritized for structure elucidation. Several data-mining techniques have been described for nontarget analysis of PFASs including characteristic fragment ion searching, Kendrick Mass Defect analysis, and direct homologous series detection.[27,34−39] Although nontarget analyses are inherently qualitative, efforts have been made to estimate concentrations of nontarget PFASs using matching data from complementary target analyses.[32]

The goals of this research were to improve our fundamental understanding of the types of PFASs that occur in fab wastewater and to assess the relative concentrations of individual PFAS species. To meet these goals, we collected wastewater from three different fabs at the photolithography step, along the conveyance path as the wastewater from photolithography is combined with other onsite wastewater, and at the point of discharge from the fab. Samples were analyzed by means of LC-HRMS and complementary target and nontarget analyses were conducted to quantify and identify PFASs, respectively, in the wastewater samples. Data were used to assess the relative abundances of individual PFAS species. This is the first study to comprehensively examine the occurrence of PFASs in electronics wastewater, and our findings are essential for developing alternative photolithography chemicals or informing the implementation of advanced wastewater treatment technologies at electronics manufacturing facilities.

MATERIALS AND METHODS

PFAS Stock Solutions. We acquired authentic standards for 25 target PFASs and 8 isotope labeled internal standards (ILISs), as detailed in Tables S1 and S2. The 25 target PFASs included 11 perfluorocarboxylic acids (PFCAs), seven perfluorosulfonic acids (PFSAs), three fluorotelomer sulfonic acids (FTSs), one perfluoroalkylsulfonamide (FOSA), two polyfluorosulfonamido acetic acid derivatives (*N*-MeFOSAA and *N*-EtFOSAA), and perfluoro-2-methyl-3-oxahexanoic acid (GenX). Stock solutions of each PFAS and ILIS were prepared in appropriate solvents at a concentration of 1 g L^{-1}, 50 mg L^{-1}, or 2 mg L^{-1} depending on the solubility of the PFAS or the ILIS. The stock solutions were used to prepare an analytical mixture containing all 25 target PFASs and an internal standard mixture containing all 8 ILISs in Milli-Q water (EDM Millipore) at a concentration of 100 μg L^{-1}. The stock solutions and mixtures were made fresh and then stored at −20 and 4 °C, respectively. Prior to usage, analytical mixtures were brought to room temperature, shaken for 30 s, vortexed for 30 s, and sonicated for 10 min to minimize the effects of precipitation, micelle formation, or adsorption during cold storage. We also acquired seven authentic standards for retrospective structural confirmation of nontarget PFASs: 2H-perfluoro-2-octenoic acid (50 mg L^{-1}, Wellington), 2H-perfluoro-2-decenoic acid (50 mg L^{-1}, Wellington), 3-perfluoropentyl propanoic acid (50 mg L^{-1}, Wellington), 3-perfluoroheptyl propanoic acid (50 mg L^{-1}, Wellington), and a fluorotelomer acid mixture containing 2-perfluorohexyl ethanoic acid, 2-perfluorooctyl ethanoic acid, and 2-perfluorodecyl ethanoic acid (2 mg L^{-1}, Wellington).

Sample Collection. We collected wastewater samples from three fabs in the United States, which we refer to as fab1, fab2, and fab3. Three sample locations were selected at each fab, as shown schematically in Figure S1. First, we collected an "upstream" wastewater sample at a location that should only contain wastewater from the photolithography step (fab1_up, fab2_up, fab3_up). Second, we collected a "midstream" wastewater sample along the conveyance path that contains wastewater from the photolithography process diluted with other onsite wastewater (fab1_mid, fab2_mid, fab3_mid). Third, we collected a "downstream" sample at the point of discharge from each of the fabs (fab1_down, fab2_down, fab3_down); fab1 discharges wastewater to a stream and fab2 and fab3 discharge wastewater to publicly owned treatment works. Duplicate samples were collected at each of the selected sampling locations in new 1 L high-density-polyethylene (HDPE) bottles; one sample bottle contained 5 g L^{-1} of a Trizma (Sigma-Aldrich) buffering reagent as suggested by EPA method 537.1 and the other sample bottle contained no reagent. Field blanks were collected from fab1 and fab2, and three tap water samples were collected for quality control purposes in fab3. Samples were mostly collected as grab samples from conveyance lines that had been flushed for several minutes, but the fab3_up sample was collected as a time-composite sample using infrastructure that was available at fab3. All samples were sealed with parafilm, packed in ice, and shipped immediately to our laboratory where they were stored at 4 °C for no more than 2 days until sample preparation and analysis.

Target Analysis. We used 12 mL polypropylene syringes and 0.45 μm cellulose acetate membrane syringe filters (Restek) to filter 10 mL aliquots of each sample with no buffering reagent into polypropylene beakers; control experiments demonstrated recoveries of the quantified PFCAs and PFSAs between 80 and 120% with this approach. We then diluted each sample up to 25-fold with Milli-Q water to create a series of prepared samples with varying target PFAS concentrations to ensure that the acquired data was within the range of our calibration curve. We transferred 8 mL of each prepared sample into 10 mL sample vials and spiked them with 20 μL of the ILIS mixture at a concentration of 40 μg L^{-1}. All samples were prepared in triplicate at each dilution level. Prepared samples were then measured by means of LC-HRMS (QExactive hybrid quadrupole-orbitrap, ThermoFisher Scientific) using a previously described analytical method.[40] Briefly, the mobile phase consisted of (A) LC-MS grade water amended with 20 mM ammonium acetate and (B) LC-MS grade methanol. Samples were injected at 5 mL volumes onto a Hypersil Gold dC18 12 μm 2.1 × 20 mm^2 trap column (ThermoFisher Scientific) and were eluted onto an Atlantis dC18 5 μm 2.1 × 150 mm^2 analytical column (Waters) at 25 °C with a pump delivering 300 μL min^{-1} of a mobile phase gradient starting at 40% B; the gradient program had a duration of 42.1 min and followed that described in EPA method 537.1 but was extended by 5.1 min to account for loading of the 5 mL sample onto the trap column. The mass spectrometer acquired full-scan MS data in negative ionization mode at a resolution of 140 000 over a mass (m/z) range of 150−1000 Da. Data-dependent MS2 data were collected at the exact masses of each of the 25 target PFASs. Calibration standards were prepared in Milli-Q water and spiked with 20 μL of the ILIS mixture at a concentration of 40 μg L^{-1}. The 25 target PFASs were quantified based on the ratio of the area

https://dx.doi.org/10.1021/acs.est.0c06690
Environ. Sci. Technol. 2021, 55, 2346−2356

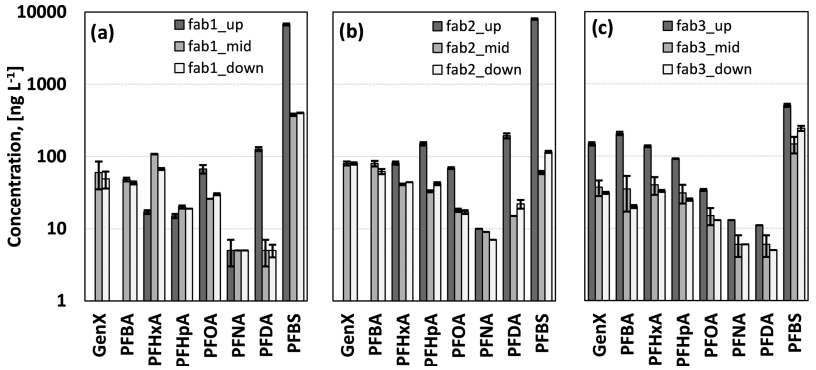

Figure 1. Average concentrations of target PFASs measured in fab wastewater from each of the fabs in upstream samples collected from the photolithography process (dark gray), along the conveyance path as the aqueous wastewater from photolithography is combined with other onsite wastewater (medium gray), and at the point of discharge from the fab (light gray). Note that fab1 and fab3 have onsite biological wastewater treatment plants prior to the point of discharge. Error bars represent the standard deviation of three technical replicates.

responses of the target PFASs to the assigned ILISs and by $1/x$ weighted linear least-squares regression. Method blanks, instrument blanks, and continuing calibration checks were included in the analyses to account for laboratory sources of contamination, sample carryover, and to verify the precision and accuracy of the calibration. Analytical details for each of the 25 target PFASs are provided in Table S3 and quality control data and limits of quantification are provided in Table S4.

Nontarget Analysis. We filtered 1 L of each wastewater sample with buffering reagent using a Nalgene filtration unit and 0.45 μm cellulose acetate filter paper (Whatman). The filtered wastewater samples were amended with 0.1% v/v ammonium acetate (1 M) and then the pH was adjusted to approximately 6.5 with 5% formic acid (ThermoFischer Scientific) and 1.4 N ammonia (Sigma-Aldrich). We performed solid phase extraction (SPE) to concentrate the PFASs in each sample using a previously described method.[41] Briefly, SPE cartridges containing styrenedivinyl-benzene (SDVB), a hydrophobic material that can extract acidic, basic, and neutral compounds (Agilent Technologies, Bond Elut-LMS, 500 mg sorbent weight), were conditioned with 15 mL of methanol (ThermoFisher Scientific) and 18 mL of Milli-Q water and then loaded with 1 L of the filtered and pH-adjusted wastewater samples or 1 L LC-MS-grade water blank samples. Analytes were eluted from the loaded cartridges using 8 mL of methanol and evaporated to 0.1 mL under a gentle stream of high-purity nitrogen gas (Air Gas). The samples were reconstituted to 1 mL with Milli-Q water and filtered through a 0.45 μm regenerated cellulose syringe filter (Restek) before being transferred to 2 mL polypropylene vials. We stored prepared samples at −20 °C until analysis. Prepared samples were measured by means of LC-HRMS using the same mobile phase composition and gradient as described in EPA method 537.1 (gradient length was 37.0 min). Samples were injected at 20 μL in triplicate directly onto an Atlantis dC18 5 μm 2.1 × 150 mm^2 analytical column (Waters) at 25 °C with a pump delivering 300 μL min^{-1} of the mobile phase. The mass spectrometer acquired full-scan MS data in negative or positive ionization modes in separate runs at a resolution of 140 000 over a mass (m/z) range of 150−2000 Da. We performed a mass calibration before every sequence and mass accuracy at m/z of 200 was always within 1 ppm. Data-dependent MS2 spectra were acquired for the three most intense ions after each full scan with dynamic exclusion set at 6 s. A data-dependent MS2 inclusion list was developed during post-acquisition data processing and used for subsequent MS2 experiments.

Post-Acquisition Data Processing. The HRMS acquisitions from the nontarget analysis were converted to *mzXML* format using MSConvert and imported into the R Statistical Software.[42] We used the *enviMass* package[43] for peak picking and the *blind* filter function to remove peaks that were present in the wastewater samples with peak areas less than 10 times the peak area in the blank samples. We then used file-wise componentization and homologous series detection to screen for evidence of putative homologous series with repeating units of CF_2, C_2F_4, CF_2O, and C_2F_4O; we note that a number of other repeating units could also be explored in this context (e.g., C_3F_6O, CF_2CH_2). Homologous series detection relied on a retention time window of 1−600 s between adjacent homologues, a m/z tolerance of 8 ppm for each homologue, and the criterion that homologous series had to contain at least three consecutive homologues; this latter criterion was implemented to limit the number of false positive homologous series selected with only two members. Homologous series identified in this way were then vetted and prioritized for structure elucidation. First, each homologue from each homologous series was examined in QualBrowser of the XCalibur software (ThermoFisher Scientific) to assess peak shape (>10 MS scans), peak intensity (>1 × 10^5), the presence of characteristic monoisotopic mass spectra, and an increasing retention time pattern with increasing m/z across the homologous series; series with one or more homologues that did not meet these quality control criteria were eliminated from further consideration. We further refined the list of homologous series by constraining the data to include only those series with m/z values within a Kendrick Mass Defect range of 0.85−1 or 0−0.15, as has been previously described.[35] The m/z values of each homologue in each of the prioritized homologous series were then added to an inclusion list and the wastewater samples were remeasured by means of LC-HRMS to acquire MS2 spectra for each homologue. We used the MS spectra and the MS2 spectra from each homologue to propose molecular formulae and to assign structures to the prioritized homologous series, as described in the Supporting Information; we used previously established criteria to assign confidence levels to all structural annotations.[44]

https://dx.doi.org/10.1021/acs.est.0c06690
Environ. Sci. Technol. 2021, 55, 2346−2356

RESULTS AND DISCUSSION

Target Analysis. Three wastewater samples were collected from each of three fabs in the United States (fab1, fab2, and fab3). We collected wastewater samples at an upstream location that should only contain wastewater from the photolithography step (fab1_up, fab2_up, fab3_up), at a midstream location along the wastewater conveyance path (fab1_mid, fab2_mid, fab3_mid), and at a downstream location at the point of discharge from each fab (fab1_down, fab2_down, fab3_down). The results of our target analysis are provided in Table S6 and are summarized in Figure 1 where we report the average and standard deviation of triplicate sample measurements of the major target PFASs that were detected. The quality control samples collected at each fab (field blanks and internal tap water) contained no target PFASs above the limit of quantitation (LOQ).

We measured 12 of the 25 target PFASs at a concentration greater than the LOQ in at least one of the fab wastewater samples (Figure S6). Six PFASs were measured in all nine wastewater samples, including perfluorohexanoic acid (PFHxA), perfluoroheptanoic acid (PFHpA), PFOA, perfluorononanoic acid (PFNA), perfluoeodecanoic acid (PFDA), and PFBS. The concentrations of the target PFASs that were measured ranged between 4 ± 1 and 8040 ± 182 ng L^{-1}. The highest concentrations were noted for PFBS in fab1_up, fab2_up, and fab3_up (6750 ± 228, 8040 ± 182, and 505 ± 25 ng L^{-1}, respectively), PFDA in fab1_up and fab2_up (127 ± 8 and 194 ± 16 ng L^{-1}, respectively), PFHpA in fab2_up (150 ± 8 ng L^{-1}), and PFHxA in fab1_mid (108 ± 1 ng L^{-1}). Perfluorobutanoic acid (PFBA), GenX, and PFHxA were also present at relatively high concentrations (206 ± 11, 148 ± 8, and 137 ± 4 ng L^{-1}, respectively) in fab3_up, the only fab in which PFBA and GenX occurred in an upstream sample. PFBA and GenX were exclusively measured in midstream and downstream samples from fab1 and fab2, which points to their use in other industrial or commercial processes within these fabs or formation from precursor chemicals.[2] We note that the fab3_up sample was collected as a time-composite sample, which may have captured sporadic loads of PFBA and GenX that were missed by grab samples collected at the other two fabs, though we cannot discount the possibility that PFBA and GenX were exclusively present in the upstream sample from fab3. Other PFASs that were quantified at low levels in one or more fab samples include PFPeA (77 ± 2 ng L^{-1} in fab3_up), PFUnA (4 ± 1 ng L^{-1} in fab1_mid and fab1_down), PFOS (8 ± 1 ng L^{-1} in fab2_up, 4 ± 0 ng L^{-1} in fab2_down), and 6:2 FTS (6 ± 2 ng L^{-1} in fab2_up).

Figure 1 demonstrates that PFBS is the dominant target PFAS in all three fabs, and that its concentration is greatest in the upstream samples. We expect that the source of PFBS is entirely related to the use of photoacid generators during photolithography.[18] We further expect that PFBS is stable along wastewater conveyance and is not transformed or adsorbed to particles during wastewater treatment.[12,28,29] Under these assumptions, we can use the changes in the PFBS concentration among the samples from each fab to estimate the amount of dilution that occurs from the upstream sample to the midstream and downstream samples. We can then compare the changes in the concentrations of the other target PFASs to the changes in the concentration of PFBS to determine whether the concentration of the other target PFASs in the midstream and downstream samples can be explained by dilution. We note that any formation of PFBS during conveyance or other sources of PFBS within the fabs would lead to an underestimate of dilution, which would make our subsequent analyses more conservative. Using this approach, we determined that the concentrations of PFHxA, PFHpA, PFOA, and PFNA in fab1_mid and fab1_down were all at least 7 times greater than we would expect based on dilution alone. This suggests that there may be other sources for these PFCAs within the fab or that they may be formed from precursors during conveyance or onsite wastewater treatment.[22−26] We likewise determined that the concentrations of PFHxA, PFHpA, PFOA, PFNA, and PFDA in fab2_mid and fab2_down were all at least 10 times greater than we would expect based on dilution alone, again suggesting additional sources or formation from precursor compounds during conveyance in fab2 (fab2 has no onsite wastewater treatment). In contrast, all of the PFCAs exhibit concentrations that would be predicted from dilution in the fab3_mid and fab3_down samples, suggesting that there are no unexpected sources of these PFCAs in fab3; we note again that the fab3_up sample was collected as a time-composite sample, which may influence this observation.

The sum totals of the target PFAS concentrations in the downstream samples from fab1, fab2, and fab3 are 623 ± 24, 394 ± 18, and 376 ± 24 ng L^{-1}, respectively. These are the concentrations in the wastewater prior to dilution in a receiving water system or with municipal wastewater. These concentrations are relatively low when compared to other known sources of PFASs to the environment. For example, total concentrations of target PFASs from a fluorochemical manufacturing plant in the Cape Fear River in North Carolina were 51 000 ng L^{-1} at the source and 700 ng L^{-1} approximately 120 km downstream.[15,45] Similarly, downstream from a fluorochemical manufacturing plant in the Netherlands, total concentrations of target PFASs were found at 876 ng L^{-1}.[13] Concentrations up to 660 000 ng L^{-1} have been identified in the Dongzhulong River in China downstream from fluorochemical manufacturing sites.[46] In raw wastewater from another manufacturing facility, PFOA alone has been measured at concentrations ranging from 1600 to 46 200 ng L^{-1}.[47] In this context, the sum concentrations of target PFASs released by the three electronics manufacturing facilities included in this study are relatively low. Nevertheless, the total concentration of target PFASs in wastewater effluent from each fab could be of concern to the environment surrounding the discharge point and some level of precaution is warranted.[8,48]

Nontarget Analysis. Because we are interested in discovering all classes of PFASs that might be present in fab wastewater, including unknown PFAS species that are used during photolithography or their transformation products, we developed a nontarget workflow to prioritize homologous series of PFASs within our HRMS acquisitions for structure elucidation. We applied our workflow to positive mode and negative mode HRMS acquisitions and screened the data for evidence of homologous series with repeating units of CF_2, C_2F_4, CF_2O, and C_2F_4O. We found no evidence of homologous series in the positive mode acquisitions. However, negative mode acquisitions provided evidence of a large number of homologous series, including identification of the PFCA, PFSA, and FTS homologous series that were included in the target analysis (we note that SPE enrichment allowed for detection of more homologues of these PFASs in the nontarget

https://dx.doi.org/10.1021/acs.est.0c06690
Environ. Sci. Technol. 2021, 55, 2346−2356

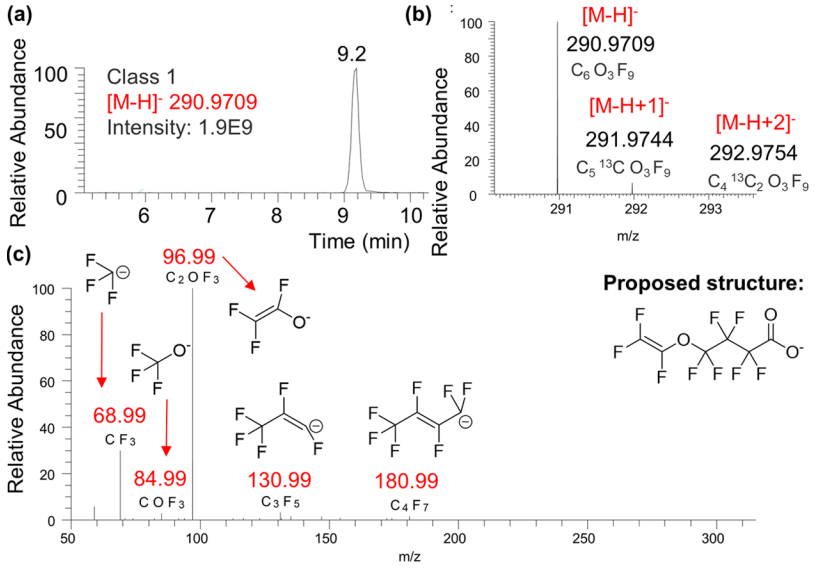

Figure 2. Analytical data supporting the structure elucidation of a nontarget PFAS. Class 1 was identified as a three-member homologous series (190.9763, 240.9735, 290.9709). The most intense member (290.9709) was measured in wastewater samples from all three fabs at a retention time of 9.2 min, as shown in (a) extracted ion chromatogram. The proposed molecular formula assignment ($C_6O_3F_9^-$) is supported by (b) MS spectra (m/z = 290.9709 for $[M - H]^-$, Δm = −0.07 ppm) and the theoretical abundance (~6%) of the ^{13}C monoisotopic mass (m/z = 291.9744 for $[M - H + 1]^-$, Δm = 0.4 ppm). The MS2 fragments (c) with masses of 68.99, 84.99, 96.99, 130.99, and 180.99 along with data from a Safety Data Sheet (SDS) for a commercially available antireflective coating support the proposed structure with a confidence of Level 2. The structural assignments for MS2 fragments with masses of 68.99, 84.99, 130.99, and 180.99 are the likely result of gas-phase rearrangements during the tandem mass spectrometry experiment.[58,59] The proposed structure results from an ester hydrolysis reaction of a known photolithography additive (see Figure 3a). Class 1 represents a homologous series of unsaturated perfluoromonoether carboxylic acids.

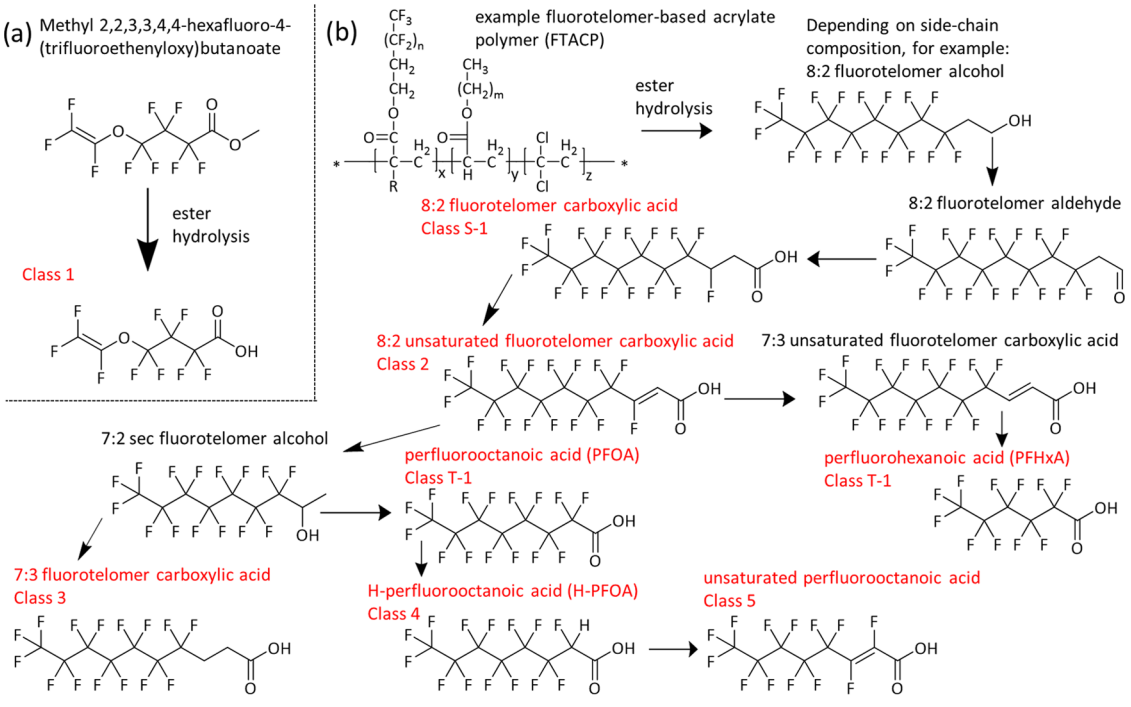

Figure 3. Reaction pathways that support the proposed structures of nontarget PFASs and proposed groups of nontarget PFASs. (a) Class 1 is proposed to arise from an ester hydrolysis reaction of methyl 2,2,3,3,4,4-hexafluoro-4-(trifluoroethenyloxy)butanoate, a known constituent of commercially available top antireflective coatings. (b) Group 2 PFASs are proposed to be related as transformation products of fluorotelomer-based acrylate polymers (FTACPs). Structures labeled in the red text represent nontarget PFASs discovered in this work. Structures labeled in the black text are proposed transformation intermediates that were not discovered in this work. Pathway adapted from several sources.[23,24,26,51]

analysis than were quantified in the target analysis). Identification of the PFCA, PFSA, and FTS homologous series provides validation that our workflow can successfully identify homologous series of PFASs. Following manual vetting of each homologue in each putative homologous series, we discovered 41 homologous series of nontarget PFASs comprising 133 homologues that were present in at least one of the wastewater samples. These included twenty homologous

https://dx.doi.org/10.1021/acs.est.0c06690
Environ. Sci. Technol. 2021, 55, 2346−2356

Table 1. List of Proposed Nontarget Homologous Series Assigned a Confidence of Level 3 or Higher

Class, Group	Chemical Structure, Class Name	Molecular Formula[a], n[b], Level	Class, Group	Chemical Structure, Class Name	Molecular Formula, n[a], Level
1 1	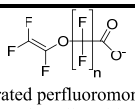 unsaturated perfluoromonoether carboxylic acids	$C_4O_3F_5^-$ 1-3 2	7 3	 unsaturated perfluoroalcohols	$C_4OF_7^-$ 2-4 2
S-1[c] 2	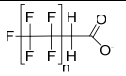 n:2 fluorotelomer carboxylic acids	$C_8H_2O_2F_{13}^-$ 3,4 1	8 4	 perfluoromonoether alcohols	$C_5O_2F_{11}^-$ 4-6 2
2 2	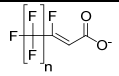 n:2 unsaturated fluorotelomer carboxylic acids	$C_6HO_2F_8^-$ 3,5-7 1	9 4	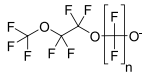 perfluorodiether alcohols	$C_6O_3F_{13}^-$ 3-6 3
3 2	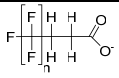 n:3 fluorotelomer carboxylic acids	$C_8H_4O_2F_{11}^-$ 5-7 1	10[d] 4	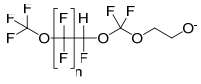 polyfluoropolyether alcohols	$C_5H_5O_4F_6^-$ 0-1 3
4 2	 H-perfluorocarboxylic acids	$C_4HO_2F_6^-$ 2-5 2	11 4	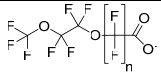 perfluoropolyether carboxylic acids	$C_5O_4F_9^-$ 1-3 2
5 2	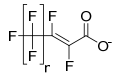 unsaturated perfluorocarboxylic acids	$C_6O_2F_9^-$ 3-8 2	12 1	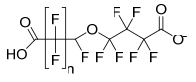 polyfluoromonoether dicarboxylic acids	$C_8H_2O_5F_{11}^-$ 2-5 3
6 3	 perfluoroalcohols	$C_3OF_7^-$ 3-5 2	13 1	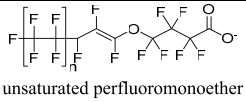 unsaturated perfluoromonoether carboxylic acids	$C_9HO_3F_{14}^-$ 1,2,3 3
14 1	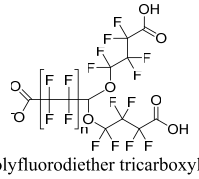 polyfluorodiether tricarboxylic acids	$C_{12}H_3O_8F_{16}^-$ 1,2,3 3	15 1	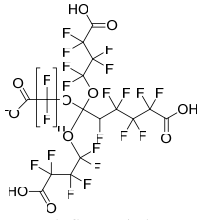 polyfluorotriether tetracarboxylic acids	$C_{18}H_4O_{11}F_{25}^-$ 3-7 3

[a]Molecular formula is of the smallest member of the homologous series that was detected. [b]n is the number of repeating units. [c]Class S-1 (for suspect) contains 2-perfluorohexyl ethanoic acid and 2-perfluorooctyl ethanoic acid, which were discovered during a retrospective suspect screening for potential intermediates of fluorotelomer-based acrylate polymer (FTACP) transformation. [d]One member of Class 10 was removed after reviewing the analytical data further, making it a two-member homologous series.

series with a CF_2 unit, six homologous series with a C_2F_4 unit, 11 homologous series with a CF_2O unit, and four homologous series with a C_2F_4O unit. Detailed information on each homologous series and homologue is provided in Tables S7 and S8.

Next, we aimed to elucidate the structures for as many of the 41 homologous series as possible. Figure 2 provides an example of how we used the analytical data to assign a structure to a homologue measured with an accurate mass of 290.9709 (referred to here as a homologue of the Class 1 homologous series). The extracted ion chromatogram (XIC), the MS spectra, and the MS2 spectra for this homologue are provided in Figure 2a–c, respectively. The XIC reveals a chromatographic peak with a retention time of 9.2 min and an intensity of 1.9×10^9 (arbitrary units). The MS spectra reveal a ^{13}C monoisotopic mass $[M - H + 1]^-$ with a theoretical abundance of 6%, which suggests a molecule that contains approximately six carbon atoms. The $[M - H + 2]^-$ adduct has a low relative abundance, suggesting that the molecule contains no sulfur (or chlorine or bromine) atoms. The accurate mass and the MS spectra of this homologue and the other two homologues in this homologous series lead to the unequivocal molecular formula of $C_6O_3F_9^-$ for this homologue. Five distinct MS2 fragments were identified for this compound at masses (m/z) of 68.99, 84.99, 96.99, 130.99, and 180.99 and the proposed structures of each fragment are provided in Figure 2c. Together, the analytical data support the proposed structure for this homologue provided in Figure 2. A subsequent review of SDSs from commercial photolithography products suggests that this is a hydrolysis product of a

https://dx.doi.org/10.1021/acs.est.0c06690
Environ. Sci. Technol. 2021, 55, 2346−2356

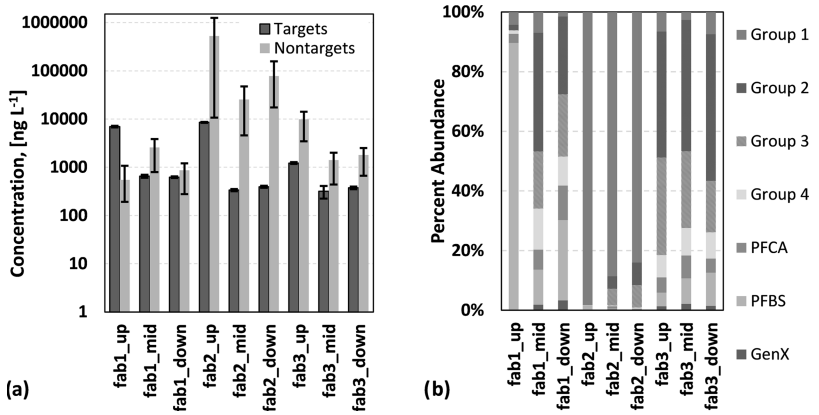

Figure 4. Sum of the average concentrations of target (measured) and nontarget (estimated) PFASs in fab wastewater collected from three fabs (a) and the relative abundance of each of the four nontarget PFAS groups along with the perfluorocarboxylic acids (PFCAs), perfluorobutane sulfonate (PFBS), and GenX (b). Error bars in (a) for target PFASs represent the standard deviation of three technical replicates. Error bars in (a) for nontarget PFASs represent the minimum and maximum estimated concentration based on three approaches to matching with target PFASs.

constituent in a widely used antireflective coating (see Figure 3a).[49] All of these data (probable structure, MS and MS2 evidence, and additional SDS support) allow us to propose structures for Class 1 with a confidence of level 2 (Table S5).

This approach to structure elucidation allowed us to propose structures for 15 of the 41 homologous series discovered with our nontarget workflow with a confidence of level 3 or higher. The structures of these 15 classes of PFASs are provided in Table 1 and the analytical details that support the structural assignments are provided in Table S7 and Figures S6−S24. The remaining 26 homologous series lacked sufficient analytical data to raise our confidence above a level 5 and the accurate masses for each homologue of these homologous series are provided in Table S8. We acquired authentic standards for two homologues of the Class 2 nontarget PFAS series (2H-perfluoro-2-octenoic acid and 2H-perfluoro-2-decenoic acid) and two homologues of the Class 3 nontarget PFAS series (3-perfluoropentyl propanoic acid and 3-perfluoroheptyl propanoic acid) and confirmed the proposed structures by matching retention times and MS2 fragments; therefore, Class 2 and Class 3 were identified with a confidence of level 1. Seven other nontarget PFAS homologous series for which a structure was proposed were identified with a confidence of level 2, meaning that all analytical data supported a single plausible structure or that database matches support the structure proposed in Table 1. The remaining six nontarget PFAS homologous series were identified with a confidence of level 3, meaning that the analytical data supports the proposed structure, but two or more isomers are possible. All homologous series identified with a confidence of level 1, 2, or 3 have proposed structures that contain only carbon, oxygen, fluorine, and hydrogen atoms and could be classified as saturated or unsaturated alcohols, ethers, and carboxylic acids. Previous studies have identified isomers of homologues of the Class 1 and Class 7 PFASs (i.e., double bond suggested in a different location)[14] and homologues of Classes 2−6, 8, and 11.[14,23,24,39,50] To the best of our knowledge, the remaining six nontarget PFAS classes (Classes 9, 10, 12−15) are reported here for the first time. The Class 12, 14, and 15 PFASs are particularly interesting because they each exhibit multiple carboxylic acid groups, which is not a common feature of previously reported PFASs.

To gain a better understanding of how the nontarget PFASs might be related to each other, we examined the occurrence and abundance patterns of each of the nontarget PFAS classes among the samples from each fab (Table S9). We were able to propose four groups of PFASs among the 15 classes based on functional groups, occurrence patterns, or transformation pathways described in the literature. Group 1 contains the Class 1 and the Class 12−15 PFASs, which share similar structures and occurrence patterns among the samples. Class 1 is proposed to arise from an ester hydrolysis reaction of methyl 2,2,3,3,4,4-hexafluoro-4-(trifluoroethenyloxy)butanoate (MHTB), a constituent of a commercially available antireflective coating (Figure 3a). This reaction yields the most abundant homologue of Class 1 (Figure 2), which is characterized by an oxy perfluoropropanoic acid appendage and is most abundant in wastewater samples collected from fab2. Class 12−15 PFASs are likewise present in greatest abundance in fab2 and their structures are also characterized by at least one oxy perfluoropropanoic acid appendage. Based on these data, we suggest that the Class 12−15 PFASs are linked to antireflective coatings that contain MHTB and are likely present as impurities or transformation products because they are not listed on the SDSs for those products. Group 2 contains the Class 2−5 PFASs along with the PFCAs (referred to as Class T-1 for target) and the Class S-1 PFASs (Table 1). We propose that these PFAS classes are related as transformation products of FTACPs as detailed in Figure 3b,[14,22−26,51] though these PFAS classes may also be derived from transformation of other types of fluorotelomer-based PFASs. Class S-1 (for suspect) was identified as a likely intermediate of the transformation of FTACPs and its presence was confirmed with a confidence of level 1 during a retrospective suspect screening of our nontarget HRMS acquisitions;[14,52] Class S-1 was not identified with our nontarget workflow because the series contains only two homologues. Group 3 contains the Class 6 and Class 7 PFASs, which are saturated and unsaturated perfluorinated alcohols. The sources of Group 3 PFASs in fab wastewater are unknown, but they could also be transformation products of FTACPs, as side chains can be attached to polymers by ester linkages and fluorinated alcohols have been reported as transformation products following base-mediated nucleophilic acyl substitution of ester linkages.[23,26] Group 4 contains the Class 8−11

https://dx.doi.org/10.1021/acs.est.0c06690
Environ. Sci. Technol. 2021, 55, 2346−2356

PFASs, which are per- and polyfluoroether alcohols and carboxylates and could also be transformation products of FTACPs following hydrolytic cleavage at the ester linkages, depending on the chemical nature of the side chain.[23,26]

The discovery of a variety of ether alcohols and ether carboxylic acids in our nontarget analysis is important because PFASs with ether bonds are persistent in the environment.[53,54] Other ether alcohols and ether carboxylic acids have been reported in water resources around the world, showing the equally ubiquitous nature of these emerging PFASs when compared to the well-known legacy PFASs.[33,50,53] Studies have also shown that some perfluoroalkyl ethers have similar bioaccumulation and toxicity potential as PFOA and other legacy PFASs and thus should be of equal concern to human health.[9,54] These recent reports all suggest that the nontarget PFASs discovered in fab wastewater may be important from an environmental health perspective and warrant further study with respect to the environmental occurrence, persistence, and toxicity.

Relative Abundance of Nontarget PFASs. To determine whether nontarget PFASs were more or less abundant than the target PFASs, we performed a semiquantification of the nontarget PFASs.[32,55,56] We matched each nontarget PFAS for which a structure was proposed with a target PFAS that had already been quantified in the target analysis (Table S6) based on either its perfluorinated chain length, the mass of the homologue, or the retention time of the homologue. We then calculated the ratio of the peak area of the nontarget PFAS and the peak area of the matched target PFAS in a given sample and multiplied that ratio by the concentration of the matched target PFAS in that sample. We finally averaged the estimated concentrations of each nontarget PFAS based on each of the three approaches for identifying a matching target PFAS. Additional details on our approach along with the full results of this semiquantification are provided in the Supporting Information and Tables S10−S12, respectively, and are summarized in Figure 4.

We found that the average estimated concentrations of 69% of the nontarget PFASs were less than 10 ng L^{-1} across all wastewater samples. However, average estimated concentrations of homologues of Classes 1, 4, 7, and 12−15 all exceeded 1000 ng L^{-1} in at least one of the wastewater samples. Figure 4a shows that the sum of the average estimated concentration of all nontarget PFASs is greater than the sum of the average concentrations of all target PFASs in eight of the nine wastewater samples (the exception is fab1_up). The fab2 wastewater samples and the fab3_up sample exhibit estimated nontarget PFAS concentrations more than an order of magnitude greater than target PFASs, though the uncertainty in the estimated concentrations of nontarget PFAS is relatively high. Figure 4b shows that the PFAS composition of wastewater from the fab1_up sample is dominated by PFBS, but the other fab1 wastewater samples contain PFAS from all groups. fab2 is dominated by nontarget PFASs from Group 1 in the fab2_up sample and Groups 1−3 in the fab2_mid and fab2_down samples. fab3 samples contain PFAS from all groups, but more than 50% of the PFAS concentrations are from Groups 2 and 3. Adding the data from the semiquantification of nontarget PFASs to the data reported for the target PFASs, the sum of the average nontarget and target PFAS concentrations in the downstream samples from fab1, fab2, and fab3 are 1490, 78 700, and 2170 ng L^{-1}, respectively.

We again used PFBS as a conservative tracer to evaluate whether the estimated concentrations of the nontarget PFASs could be explained by dilution or if there was evidence of formation or transformation. With this approach, we were able to determine that most of the nontarget PFASs exhibit higher estimated concentrations in the midstream and downstream samples than would be predicted based on dilution, suggesting possible formation from precursors during conveyance. In fab1, homologues from Classes 2, 4, 5, 6, 8, 9, 10, and 11 all exhibit concentrations greater than 10 times that would be predicted based on dilution, which suggests formation during conveyance. We also found that homologues from Classes 13−15 exhibit concentrations in downstream samples from fab2 that are more than 10 times less than what would be predicted based on dilution. This suggests that homologues from Classes 13−15 are transformed during conveyance and may result in the formation of shorter and more polar PFASs that may have escaped our detection. Homologues from Classes 1, 2, 4, 6, 7, 9, and 12 exhibit concentrations greater than 10 times what would be predicted based on dilution in fab2 suggesting formation during conveyance, and Class 1 may be plausibly formed from transformation of Classes 13−15. In contrast, all of the nontarget PFASs exhibit concentrations that would be predicted from dilution in the fab3_mid and fab3_down samples, suggesting that there is limited formation and transformation of the nontarget PFASs during conveyance in fab3. This is consistent with what we observed for the target analysis and may be influenced by the composite sampling employed for fab3_up. The results from the semiquantification of the nontarget PFASs highlight that nontarget PFASs make up a significant, if not dominant, portion of total PFASs in all three fabs. The PFBS tracer analysis also provides further insight into the potential formation or degradation of some nontarget PFASs during conveyance.

Environmental Implications. The occurrence of PFASs in the environment is of great concern for environmental and public health. It is essential to understand sources of PFASs, concentrations of legacy PFASs, and the structures of unknown PFASs. Our study was the first to comprehensively explore electronics manufacturing facilities as a source of PFASs to the environment. We found that the concentrations of legacy PFASs discharged in fab wastewater can be on the order of 100s of ng L^{-1}. This is a relatively low concentration considering wastewater discharges will be further diluted by surface water or municipal wastewater. However, we also estimated the combined concentrations of target and nontarget PFASs discharged in fab wastewater to be on the order of 1000s to 10 000s of ng L^{-1}. This was not necessarily unexpected because many studies of total organic fluorine have shown that total PFAS concentrations are at least 10 times higher than the sum of target PFASs.[27,33,53,57] However, this does reinforce the idea that PFAS monitoring should incorporate complementary target and nontarget analyses or otherwise include measures of total organic fluorine to accurately assess PFAS abundance and potential environmental impacts. These data also support the recent push by policymakers to regulate total PFASs, rather than individual compounds, underscoring the importance of total PFAS concentration monitoring.[48]

We proposed structures for 15 classes of nontarget PFASs comprised of 53 homologues, of which 6 classes of nontarget PFASs and 21 homologues are reported in this study for the first time. Therefore, this study contributes to the growing

https://dx.doi.org/10.1021/acs.est.0c06690
Environ. Sci. Technol. 2021, 55, 2346−2356

literature on unknown PFASs that may occur in the environment. Little is known about the PFASs discovered in this study, and future work should focus on the occurrence, persistence, and toxicity of these PFASs. Because some of the nontarget PFASs we identified are linked to photolithography chemicals, we expect to use these data to further evaluate electronics manufacturing facilities as sources of PFASs in the environment.

■ ASSOCIATED CONTENT

Supporting Information

The Supporting Information is available free of charge at https://pubs.acs.org/doi/10.1021/acs.est.0c06690.

Details on PFAS standards, sample locations, analytical data for target PFASs, quality control data for target PFASs, details on structure elucidation, analytical data for nontarget PFASs, and semiquantification of nontarget PFASs (PDF)

■ AUTHOR INFORMATION

Corresponding Author

Damian E. Helbling − *School of Civil and Environmental Engineering, Cornell University, Ithaca, New York 14853, United States;* orcid.org/0000-0003-2588-145X; Phone: [redacted]; Email: damian.helbling@cornell.edu; Fax: [redacted]

Authors

Paige Jacob − *School of Civil and Environmental Engineering, Cornell University, Ithaca, New York 14853, United States*

Krista A. Barzen-Hanson − *Elmira College, Elmira, New York 14901, United States*

Complete contact information is available at: https://pubs.acs.org/10.1021/acs.est.0c06690

Notes

The authors declare no competing financial interest.

■ ACKNOWLEDGMENTS

This project was supported by a grant from the Semiconductor Research Corporation (SRC) with a project identifier of Task 2818.002.

■ REFERENCES

(1) Hu, X. C.; Andrews, D. Q.; Lindstrom, A. B.; Bruton, T. A.; Schaider, L. A.; Grandjean, P.; Lohmann, R.; Carignan, C. C.; Blum, A.; Balan, S. A.; Higgins, C. P.; Sunderland, E. M. Detection of Poly- and Perfluoroalkyl Substances (PFASs) in U.S. Drinking Water Linked to Industrial Sites, Military Fire Training Areas, and Wastewater Treatment Plants. *Environ. Sci. Technol. Lett.* **2016**, *3*, 344−350.

(2) Wang, Z.; DeWitt, J. C.; Higgins, C. P.; Cousins, I. T. A Never-Ending Story of Per- and Polyfluoroalkyl Substances (PFASs)? *Environ. Sci. Technol.* **2017**, *51*, 2508−2518.

(3) Pan, Y.; Zhang, H.; Cui, Q.; Sheng, N.; Yeung, L. W. Y.; Sun, Y.; Guo, Y.; Dai, J. Worldwide Distribution of Novel Perfluoroether Carboxylic and Sulfonic Acids in Surface Water. *Environ. Sci. Technol.* **2018**, *52*, 7621−7629.

(4) *Occurrence and Use of Highly Fluorinated Substances and Alternatives*; KEMI: Stockholm, 2015.

(5) Houtz, E. F.; Higgins, C. P.; Field, J. A.; Sedlak, D. L. Persistence of Perfluoroalkyl Acid Precursors in AFFF-Impacted Groundwater and Soil. *Environ. Sci. Technol.* **2013**, *47*, 8187−8195.

(6) Pan, Y.; Zhang, H.; Cui, Q.; Sheng, N.; Yeung, L. W. Y.; Guo, Y.; Sun, Y.; Dai, J. First Report on the Occurrence and Bioaccumulation of Hexafluoropropylene Oxide Trimer Acid: An Emerging Concern. *Environ. Sci. Technol.* **2017**, *51*, 9553−9560.

(7) Caverly Rae, J. M.; Craig, L.; Slone, T. W.; Frame, S. R.; Buxton, L. W.; Kennedy, G. L. Evaluation of Chronic Toxicity and Carcinogenicity of Ammonium 2,3,3,3-Tetrafluoro-2-(Heptafluoropropoxy)-Propanoate in Sprague−Dawley Rats. *Toxicol. Rep.* **2015**, *2*, 939−949.

(8) Borg, D.; Lund, B.-O.; Lindquist, N.-G.; Håkansson, H. Cumulative Health Risk Assessment of 17 Perfluoroalkylated and Polyfluoroalkylated Substances (PFASs) in the Swedish Population. *Environ. Int.* **2013**, *59*, 112−123.

(9) Dewitt, J. C., Ed. *Toxicological Effects of Perfluoroalkyl and Polyfluoroalkyl Substances*, 1st ed.; Humana Press, 2015.

(10) Place, B. J.; Field, J. A. Identification of Novel Fluorochemicals in Aqueous Film-Forming Foams Used by the US Military. *Environ. Sci. Technol.* **2012**, *46*, 7120−7127.

(11) Lang, J. R.; Allred, B. M.; Field, J. A.; Levis, J. W.; Barlaz, M. A. National Estimate of Per- and Polyfluoroalkyl Substance (PFAS) Release to U.S. Municipal Landfill Leachate. *Environ. Sci. Technol.* **2017**, *51*, 2197−2205.

(12) Arvaniti, O. S.; Stasinakis, A. S. Review on the Occurrence, Fate and Removal of Perfluorinated Compounds during Wastewater Treatment. *Sci. Total Environ.* **2015**, *524*−*525*, 81−92.

(13) Gebbink, W. A.; van Asseldonk, L.; van Leeuwen, S. P. J. Presence of Emerging Per- and Polyfluoroalkyl Substances (PFASs) in River and Drinking Water near a Fluorochemical Production Plant in the Netherlands. *Environ. Sci. Technol.* **2017**, *51*, 11057−11065.

(14) Wang, Y.; Yu, N.; Zhu, X.; Guo, H.; Jiang, J.; Wang, X.; Shi, W.; Wu, J.; Yu, H.; Wei, S. Suspect and Nontarget Screening of Per- and Polyfluoroalkyl Substances in Wastewater from a Fluorochemical Manufacturing Park. *Environ. Sci. Technol.* **2018**, *52*, 11007−11016.

(15) Sun, M.; Arevalo, E.; Strynar, M.; Lindstrom, A.; Richardson, M.; Kearns, B.; Pickett, A.; Smith, C.; Knappe, D. R. U. Legacy and Emerging Perfluoroalkyl Substances Are Important Drinking Water Contaminants in the Cape Fear River Watershed of North Carolina. *Environ. Sci. Technol. Lett.* **2016**, *3*, 415−419.

(16) Mueller, R.; Yingling, V. *History and Use of Per- and Polyfluoroalkyl Substances (PFAS)*, 2020.

(17) Brunner, T. A. Why Optical Lithography Will Live Forever. *J. Vac. Sci. Technol., B* **2003**, *21*, 2632.

(18) *Emission Scenario Document on Photoresist Use in Semiconductor Manufcaturing*; OECD, 2010.

(19) Tang, C. Y.; Fu, Q. S.; Robertson, A. P.; Criddle, C. S.; Leckie, J. O. Use of Reverse Osmosis Membranes to Remove Perfluorooctane Sulfonate (PFOS) from Semiconductor Wastewater. *Environ. Sci. Technol.* **2006**, *40*, 7343−7349.

(20) Ayothi, R.; Yi; Cao, H. B.; Yueh, W.; Putna, S.; Ober, C. K. Arylonium Photoacid Generators Containing Environmentally Compatible Aryloxyperfluoroalkanesulfonate Groups. *Chem. Mater.* **2007**, *19*, 1434−1444.

(21) Lee, K.; Jockusch, S.; Turro, N. J.; French, R. H.; Wheland, R. C.; Lemon, M. F.; Braun, A. M.; Widerschpan, T.; Dixon, D. A.; Li, J.; Ivan, M.; Zimmerman, P. 157 Nm Pellicles (Thin Films) for Photolithography: Mechanistic Investigation of the VUV and UV-C Photolysis of Fluorocarbons. *J. Am. Chem. Soc.* **2005**, *127*, 8320−8327.

(22) Rankin, K.; Lee, H.; Tseng, P. J.; Mabury, S. A. Investigating the Biodegradability of a Fluorotelomer-Based Acrylate Polymer in a Soil−Plant Microcosm by Indirect and Direct Analysis. *Environ. Sci. Technol.* **2014**, *48*, 12783−12790.

(23) Washington, J. W.; Jenkins, T. M.; Rankin, K.; Naile, J. E. Decades-Scale Degradation of Commercial, Side-Chain, Fluorotelomer-Based Polymers in Soils and Water. *Environ. Sci. Technol.* **2015**, *49*, 915−923.

(24) Washington, J. W.; Jenkins, T. M.; Weber, E. J. Identification of Unsaturated and 2H Polyfluorocarboxylate Homologous Series and

Their Detection in Environmental Samples and as Polymer Degradation Products. *Environ. Sci. Technol.* **2015**, *49*, 13256−13263.
(25) Schellenberger, S.; Jönsson, C.; Mellin, P.; Levenstam, O. A.; Liagkouridis, I.; Ribbenstedt, A.; Hanning, A.-C.; Schultes, L.; Plassmann, M. M.; Persson, C.; Cousins, I. T.; Benskin, J. P. Release of Side-Chain Fluorinated Polymer-Containing Microplastic Fibers from Functional Textiles During Washing and First Estimates of Perfluoroalkyl Acid Emissions. *Environ. Sci. Technol.* **2019**, *53*, 14329−14338.
(26) Washington, J. W.; Jenkins, T. M. Abiotic Hydrolysis of Fluorotelomer-Based Polymers as a Source of Perfluorocarboxylates at the Global Scale. *Environ. Sci. Technol.* **2015**, *49*, 14129−14135.
(27) Dubocq, F.; Wang, T.; Yeung, L. W. Y.; Sjöberg, V.; Kärrman, A. Characterization of the Chemical Contents of Fluorinated and Fluorine-Free Firefighting Foams Using a Novel Workflow Combining Nontarget Screening and Total Fluorine Analysis. *Environ. Sci. Technol.* **2020**, *54*, 245−254.
(28) Houtz, E.; Wang, M.; Park, J.-S. Identification and Fate of Aqueous Film Forming Foam Derived Per- and Polyfluoroalkyl Substances in a Wastewater Treatment Plant. *Environ. Sci. Technol.* **2018**, *52*, 13212−13221.
(29) Pan, C.-G.; Liu, Y.-S.; Ying, G.-G. Perfluoroalkyl Substances (PFASs) in Wastewater Treatment Plants and Drinking Water Treatment Plants: Removal Efficiency and Exposure Risk. *Water Res.* **2016**, *106*, 562−570.
(30) Krauss, M.; Singer, H.; Hollender, J. LC-High Resolution MS in Environmental Analysis: From Target Screening to the Identification of Unknowns. *Anal. Bioanal. Chem.* **2010**, *397*, 943−951.
(31) Barzen-Hanson, K. A.; Field, J. A. Discovery and Implications of C2 and C3 Perfluoroalkyl Sulfonates in Aqueous Film-Forming Foams and Groundwater. *Environ. Sci. Technol. Lett.* **2015**, *2*, 95−99.
(32) Li, Y.; Yu, N.; Du, L.; Shi, W.; Yu, H.; Song, M.; Wei, S. Transplacental Transfer of Per- and Polyfluoroalkyl Substances Identified in Paired Maternal and Cord Sera Using Suspect and Nontarget Screening. *Environ. Sci. Technol.* **2020**, *54*, 3407−3416.
(33) Chen, H.; Zhang, L.; Li, M.; Yao, Y.; Zhao, Z.; Munoz, G.; Sun, H. Per- and Polyfluoroalkyl Substances (PFASs) in Precipitation from Mainland China: Contributions of Unknown Precursors and Short-Chain (C2−C3) Perfluoroalkyl Carboxylic Acids. *Water Res.* **2019**, *153*, 169−177.
(34) Koelmel, J. P.; Paige, M. K.; Aristizabal-Henao, J. J.; Robey, N. M.; Nason, S. L.; Stelben, P. J.; Li, Y.; Kroeger, N. M.; Napolitano, M. P.; Savvaides, T.; Vasiliou, V.; Rostkowski, P.; Garrett, T. J.; Lin, E.; Deigl, C.; Jobst, K.; Townsend, T. G.; Godri Pollitt, K. J.; Bowden, J. A. Toward Comprehensive Per- and Polyfluoroalkyl Substances Annotation Using FluoroMatch Software and Intelligent High-Resolution Tandem Mass Spectrometry Acquisition. *Anal. Chem.* **2020**, *92*, 11186−11194.
(35) Barzen-Hanson, K. A.; Roberts, S. C.; Choyke, S.; Oetjen, K.; McAlees, A.; Riddell, N.; McCrindle, R.; Ferguson, P. L.; Higgins, C. P.; Field, J. A. Discovery of 40 Classes of Per- and Polyfluoroalkyl Substances in Historical Aqueous Film-Forming Foams (AFFFs) and AFFF-Impacted Groundwater. *Environ. Sci. Technol.* **2017**, *51*, 2047−2057.
(36) Dimzon, I. K.; Trier, X.; Frömel, T.; Helmus, R.; Knepper, T. P.; de Voogt, P. High Resolution Mass Spectrometry of Polyfluorinated Polyether-Based Formulation. *J. Am. Soc. Mass Spectrom.* **2016**, *27*, 309−318.
(37) Myers, A. L.; Jobst, K. J.; Mabury, S. A.; Reiner, E. J. Using Mass Defect Plots as a Discovery Tool to Identify Novel Fluoropolymer Thermal Decomposition Products. *J. Mass Spectrom.* **2014**, *49*, 291−296.
(38) Washington, J. W.; Rosal, C. G.; McCord, J. P.; Strynar, M. J.; Lindstrom, A. B.; Bergman, E. L.; Goodrow, S. M.; Tadesse, H. K.; Pilant, A. N.; Washington, B. J.; Davis, M. J.; Stuart, B. G.; Jenkins, T. M. Nontargeted Mass-Spectral Detection of Chloroperfluoropolyether Carboxylates in New Jersey Soils. *Science* **2020**, *368*, 1103−1107.
(39) Wang, X.; Yu, N.; Qian, Y.; Shi, W.; Zhang, X.; Geng, J.; Yu, H.; Wei, S. Non-Target and Suspect Screening of per- and Polyfluoroalkyl Substances in Chinese Municipal Wastewater Treatment Plants. *Water Res.* **2020**, *183*, No. 115989.
(40) Wu, C.; Klemes, M. J.; Trang, B.; Dichtel, W. R.; Helbling, D. E. Exploring the Factors That Influence the Adsorption of Anionic PFAS on Conventional and Emerging Adsorbents in Aquatic Matrices. *Water Res.* **2020**, *182*, No. 115950.
(41) Shoemaker, J. A.; Grimmett, P. E.; Boutin, B. K. *Method 537. Determination of Selected Perfluorinated Alkyl Acids in Drinking Water by Solid Phase Extraction and Liquid Chromatography/Tandem Mass Spectrometry (LC/MS/MS)*, Version 1.1; U.S. EPA: Cincinnati, OH, 2009.
(42) R Core Team. *R: A Language and Environment for Statistical Computing*; R Foundation for Statistical Computing: Vienna, Austria, 2008.
(43) Loos, M. *EnviMass Beta Version 3.1. Zenodo*, 2016.
(44) Schymanski, E. L.; Jeon, J.; Gulde, R.; Fenner, K.; Ruff, M.; Singer, H. P.; Hollender, J. Identifying Small Molecules via High Resolution Mass Spectrometry: Communicating Confidence. *Environ. Sci. Technol.* **2014**, *48*, 2097−2098.
(45) Strynar, M.; Dagnino, S.; McMahen, R.; Liang, S.; Lindstrom, A.; Andersen, E.; McMillan, L.; Thurman, M.; Ferrer, I.; Ball, C. Identification of Novel Perfluoroalkyl Ether Carboxylic Acids (PFECAs) and Sulfonic Acids (PFESAs) in Natural Waters Using Accurate Mass Time-of-Flight Mass Spectrometry (TOFMS). *Environ. Sci. Technol.* **2015**, *49*, 11622−11630.
(46) Heydebreck, F.; Tang, J.; Xie, Z.; Ebinghaus, R. Alternative and Legacy Perfluoroalkyl Substances: Differences between European and Chinese River/Estuary Systems. *Environ. Sci. Technol.* **2015**, *49*, 8386−8395.
(47) Zheng, P.; Liu, M.; Yin, H.; Shen, L.; Wang, Y.; Wu, Q. Analysis of 58 Poly-/Perfluoroalkyl Substances and Their Occurrence in Surface Water in a High-Technology Industrial Park. *Environ. Pollut.* **2020**, *267*, No. 115381.
(48) Kwiatkowski, C. F.; Andrews, D. Q.; Birnbaum, L. S.; Bruton, T. A.; DeWitt, J. C.; Knappe, D. R. U.; Maffini, M. V.; Miller, M. F.; Pelch, K. E.; Reade, A.; Soehl, A.; Trier, X.; Venier, M.; Wagner, C. C.; Wang, Z.; Blum, A. Scientific Basis for Managing PFAS as a Chemical Class. *Environ. Sci. Technol. Lett.* **2020**, *7*, 532−543.
(49) Merck. *MSDS for AZ Aquatar VIII-45A. Safety Data Sheet, 1.0*, 2018; pp 1−18.
(50) McCord, J.; Strynar, M. Identification of Per- and Polyfluoroalkyl Substances in the Cape Fear River by High Resolution Mass Spectrometry and Nontargeted Screening. *Environ. Sci. Technol.* **2019**, *53*, 4717−4727.
(51) Li, L.; Liu, J.; Hu, J.; Wania, F. Degradation of Fluorotelomer-Based Polymers Contributes to the Global Occurrence of Fluorotelomer Alcohol and Perfluoroalkyl Carboxylates: A Combined Dynamic Substance Flow and Environmental Fate Modeling Analysis. *Environ. Sci. Technol.* **2017**, *51*, 4461−4470.
(52) Pochodylo, A. L.; Helbling, D. E. Emerging Investigators Series: Prioritization of Suspect Hits in a Sensitive Suspect Screening Workflow for Comprehensive Micropollutant Characterization in Environmental Samples. *Environ. Sci. Water Res. Technol.* **2017**, *3*, 54−65.
(53) Zhang, C.; Hopkins, Z. R.; McCord, J.; Strynar, M. J.; Knappe, D. R. U. Fate of Per- and Polyfluoroalkyl Ether Acids in the Total Oxidizable Precursor Assay and Implications for the Analysis of Impacted Water. *Environ. Sci. Technol. Lett.* **2019**, *6*, 662−668.
(54) Wang, Z.; Cousins, I. T.; Scheringer, M.; Hungerbuehler, K. Hazard Assessment of Fluorinated Alternatives to Long-Chain Perfluoroalkyl Acids (PFAAs) and Their Precursors: Status Quo, Ongoing Challenges and Possible Solutions. *Environ. Int.* **2015**, *75*, 172−179.
(55) Allred, B. M.; Lang, J. R.; Barlaz, M. A.; Field, J. A. Orthogonal Zirconium Diol/C18 Liquid Chromatography−Tandem Mass Spectrometry Analysis of Poly and Perfluoroalkyl Substances in Landfill Leachate. *J. Chromatogr. A* **2014**, *1359*, 202−211.

https://dx.doi.org/10.1021/acs.est.0c06690
Environ. Sci. Technol. 2021, 55, 2346−2356

(56) Backe, W. J.; Day, T. C.; Field, J. A. Zwitterionic, Cationic, and Anionic Fluorinated Chemicals in Aqueous Film Forming Foam Formulations and Groundwater from U.S. Military Bases by Nonaqueous Large-Volume Injection HPLC-MS/MS. *Environ. Sci. Technol.* **2013**, *47*, 5226−5234.
(57) Schaider, L. A.; Balan, S. A.; Blum, A.; Andrews, D. Q.; Strynar, M. J.; Dickinson, M. E.; Lunderberg, D. M.; Lang, J. R.; Peaslee, G. F. Fluorinated Compounds in U.S. Fast Food Packaging. *Environ. Sci. Technol. Lett.* **2017**, *4*, 105−111.
(58) Gross, J. H. *Mass Spectrometry*, 2nd ed.; Springer: Heidelberg, 2004.
(59) Guarini, A.; Guglielmetti, G.; Donegani, I. G.; Fauser, V.; Analítica, C.; Guarda, P.; Marchionni, G.; Centro, R.; Ausimont, S. Characterization of Perfluoropolyethers by Desorption Chemical Ionization and Tandem Mass Spectrometry. *Anal. Chem.* **1993**, *65*, 970−975.

https://dx.doi.org/10.1021/acs.est.0c06690
Environ. Sci. Technol. 2021, 55, 2346−2356